Catalysis Today 149 (2010) 380–387

Contents lists available at ScienceDirect

Catalysis Today

journal homepage: www.elsevier.com/locate/cattod

Transient study of the dry reforming of methane over Pt supported on different γ-Al_2O_3

M. García-Diéguez, I.S. Pieta, M.C. Herrera, M.A. Larrubia, I. Malpartida, L.J. Alemany *

Departamento de Ingeniería Química, Facultad de Ciencias, Campus Universitario de Teatinos, Universidad de Málaga, E-29071 Málaga, Spain

ARTICLE INFO

Article history:
Available online 4 September 2009

Keywords:
Dry reforming
Transient Response Method (TRM)
Methane
Alumina
DRIFT-MS
Natural gas conversion

ABSTRACT

CO_2 reforming of methane has been studied over Pt/Al_2O_3 model catalysts in a temperature range of 600–800 °C using steady-state and transient methods (Transient Response Method (TRM) and DRIFT-MS). Pt-supported catalysts were prepared using two different alumina (γ-Al_2O_3(S) Sasol-Puralox and a synthesized γ-Al_2O_3(N) with nanofibrous structure). Catalysts and supports were characterized by conventional methods (XRD, TEM, A_{BET}, XPS) before and after reaction. Pt^0 species are present in the catalysts, with a higher relative contribution for the catalyst that has a nanostructured support. Pt/γ-Al_2O_3(N) catalyst presented the best performance in reactivity and showed a low rate of carbon formation and a minimal water production. From TRM and DRIFT-MS results it can be concluded that, when CO_2 and CH_4 are fed separately into the reaction system, they are activated over the catalytic surface. Besides, when both reactants are fed contemporaneously the presence of CH_X species promotes the CO_2 activation that is responsible for the reforming reaction.

1. Introduction

Reforming of CH_4 with CO_2 is an attractive transformation due to the production of *syngas* with a low H_2/CO ratio, suitable for oxo-synthesis processes. Additionally, CH_4 and CO_2 are harmful greenhouse gases that can be converted into valuable chemicals [1–5]. Ni-based catalysts are known as common catalysts for this endothermic reaction; the principal obstacle to their industrial application is the relevant coke deposition, which results in the catalyst deactivation [1,2,6,7]. Dry reforming requires the use of stable and effective catalysts, resistant to coking; hence investigations should be focused on the metal activity, the resistance to coke formation and the type of the support that improves the catalyst efficiency [2,8,9]. Furthermore, to develop an appropriate catalyst it is also important to analyze the mechanism pathway for the reforming reaction. Pt-alumina supported catalysts seem to be interesting catalysts for dry reforming, because they have shown a longer life, better selectivity and higher resistance to coking than other Ni-base catalysts tested for CO_2-reforming of methane in a model gas stream. It is well known that, apart from coke deposition, at least two factors can contribute to catalyst deactivation such as sintering and poisoning by species coming from the support. An increase of the metal dispersion and the presence of OH^- superficial groups seem to favour the formation of intermediate carbonaceous species that are more reactive, thus limiting the catalyst deactivation.

Hu and Ruckenstein [10] studied the effect of the support on the performance of Rh-based catalysts in the methane dry reforming and they found that the most promising supports for this reaction are irreducible oxides such as Al_2O_3 and MgO, which can normally be regarded as highly inert chemicals; providing better H_2 and CO yields than the reducible ones. Al_2O_3 has proved to be an effective support; however, its dispersion capacity, superficial interaction and overall reactivity depend on the conditions used during the preparation process [11]. This is especially remarkable when highly dispersed metals, such as Pt-supported on Al_2O_3, are used for structure-sensitive reactions. Moreover, at higher temperatures Al_2O_3 behaves as an N-type semiconductor, increasing the electron density when a metal is incorporated. The characteristics of Al_2O_3 are also relevant because of their acidic properties.

Different mechanism pathways have been established for the formation of CO and H_2. Bradford and Vannice [12] studied the kinetics of CO_2 dry reforming over Pt-supported catalysts. They observed that CH_4 is reversibly activated over Pt producing CH_X species and H_2. They also proposed that CO_2 activation is promoted by hydrogen adsorbed over the catalyst surface to form adsorbed CO and OH. The CH_X species react with CO_2 dissociation fragments to form CH_XO species, which irreversibly decompose to produce CO and H_2. O'Connor et al. [3] proposed a reaction scheme for the dry reforming over a Pt/Al_2O_3 catalyst. They fundamentally, reported that: (i) CH_4 reacts via decomposition over the free Pt sites; (ii) CO_2 activation is reversible and it is

* Corresponding author. Tel.: +34 952131919; fax: +34 952131919.
E-mail address: luijo@uma.es (L.J. Alemany).

0920-5861/$ – see front matter © 2009 Published by Elsevier B.V.
doi:10.1016/j.cattod.2009.07.099

assisted by hydrogen to form adsorbed CO and OH, being this step the slowest one; (iii) the alumina hydroxyl groups participate in the reaction mechanism.

Ferreira-Aparacio et al. [4] studied the CO_2 reforming of CH_4 over Ru supported catalysts; they found that CO_2 is activated on Ru and the CO formed comes from dissociation and from surface carbon oxidation. In addition, they observed that CH_4 activation occurs over Ru and it is an irreversible cracking considered as a property of the noble metals. Maestri et al. [13] made a microkinetic analysis of the dry and steam reforming. They reported that CH_4 consumption proceeds via pyrolysis and carbon oxidation by superficial OH. CO_2 activation is due to H adsorbed and the role of the CO_2 is to provide the main oxidizer.

In the present paper physicochemical and catalytic properties of two Pt/γ-Al_2O_3 model catalysts are studied towards carbon dioxide reforming of methane. In order to understand the activation process of CO_2 and CH_4, Transient Response Method (TRM-runs) and DRIFT-MS studies were performed. Transient studies have proved to be a powerful tool in elucidating reaction mechanisms [3,4,14,15]. Experiments in steady state were also performed for comparative purposes.

2. Experimental

2.1. Catalysts preparation

A commercial γ-Al_2O_3 (Sasol-Puralox SCCa-5/200) supplied by Sasol (denoted as γ-Al_2O_3(S), A_{BET} = 160 m^2/g, V_P = 0.7 cm^3/g) and a synthesized nanofibrous alumina (denoted as γ-Al_2O_3(N), A_{BET} = 300 m^2/g, V_P = 2 cm^3/g) were used as supports. The nanostructured alumina was synthesized as is described in detail in [16]. An aqueous $NaAlO_2$ solution was added dropwise to 5N acetic acid solution. The precipitated obtained was decanted, filtrated and washed with water. The white powder was dried overnight at 100 °C and subsequently mixed with a non-ionic surfactant (Tergitol 15-TS-5, Sigma) using a ratio of Tergitol/Al = 0.5. The mixture was maintained in an autoclave for 72 h at 100 °C and later calcined at 500 °C for 20 h. Before the catalysts preparation, both of the supports were calcined in air at 800 °C during 2 h (10 °C/min). Catalysts were prepared by incipient wetness impregnation of the supports using diaminedinitroplatinum(II) ($Pt(NH_3)_2(NO_2)_2$) as precursor. The Pt load was 0.4 at/nm^2 of support, expressed in terms of atomic superficial density. The materials were dried at 100 °C overnight and after calcined in air at 600 °C during 2 h. Catalysts and supports were characterized, before and after reaction, by XRD, XPS, N_2 adsorption–desorption and TEM.

2.2. Characterization

X-ray powder diffraction data have been recorded with an X'Pert MPD PRO diffractometer (PANalytical) using Cu Kα_1 radiation (λ = 1.54059 Å) and a Ge(1 1 1) primary monochromator. The X-ray tube worked at 45 kV and 35 mA. The measurements were done from 10° to 70° (2θ).

X-ray photoelectron spectra were recorded on a Physical Electronic 5701 equipped with a PHI 10-360 analyzer using the Mg Kα X-ray source. Binding energy (BE) values were referred to the C_{1s} peak (284.8 eV) from the adventitious contamination layer during data processing of the XPS spectra. All deconvolutions of experimental curves were done with Gaussian and Lorenzian line fitting of varying proportions (30–80%).

N_2 adsorption–desorption isotherms were registered at −196 °C using a Beckman Coulter SA3100 Surface Area Analyzer. Before the analysis, the samples were outgassed in vacuum (1.10^{-3} Pa) for 5 h at 180 °C. The specific surface area was obtained by the BET equation and the pore volume by the BJH method. TEM images were taken with a Philips CM 200 of 200 kV; the samples were prepared using ethanol as dispersant.

2.3. Reactivity

Steady-state experiments were carried out in a Microactivity-Reference reaction system from PID at atmospheric pressure in a temperature range between 500 and 700 °C. A tubular fixed bed stainless steel reactor (i.d. 9 mm) with 100 mg of catalyst was employed. The total gas flow rate was kept constant at 50 N cm^3/min with stoichiometric composition diluted in He (CH_4/CO_2/He = 20/20/60). The space velocity and the contact time were 6000 h^{-1} and 0.8 g h mol^{-1}, respectively. Before reaction, catalysts were activated *in situ* with H_2 (3% in He, 30 ml/min) at 700 °C during 2 h. The reaction temperature was measured with a thermocouple placed in the reactor bed. The reactor effluent was analyzed by GC (Agilent 5890D) equipped with TCD and FID detectors.

TRM-runs were performed following the Transient Response Method (TRM-MS). The transient response for consecutive rectangular pulses was analyzed in a flow reaction system with an automatic valve at the inlet, which allows instant changes of the feed composition gases. The catalyst was activated before reaction at the same conditions as in the steady-state experiments. The values of space velocity and the contact time were similar to those employed in the steady-state runs (GHSV = 5500 h^{-1} and W/F_T = 0.9 g h mol^{-1}). The outlet gases were analyzed by Mass Spectrometry (MS, Pfeiffer Prisma, QMS 200). Two different tests (denoted as Types I and II) were carried out switching the valve each 5 min to change the feed composition from CH_4/He/Ar to CO_2/He/Ar and from CH_4/CO_2/He/Ar to He for the experiments Types I and II, respectively. For both experiments the inlet gas composition was stoichiometric CH_4/CO_2 = 1/1 and diluted in He. Ar was used as a tracer to establish the beginning and the end of each pulse. The following m/e values were selected: 2 (H_2), 18 (H_2O), 15 (CH_4), 44 (CO_2), 28 (CO) and 40 (Ar). The contribution from other specie than the indicated was subtracted, as well as the background. The signals of the reaction products were normalized considering the maximum registered during the TRM experiments for each catalyst. The CH_4 and CO_2 signals were normalized with respect to the maximum registered at room temperature without the catalyst. Each of the experiments (Types I and II at the selected temperature) consisted of 40 pulses, being the first one of CO_2 in the Experiments Type I and CO_2–CH_4 in the Experiments Type II.

DRIFT-MS runs were performed in a high temperature reaction chamber (Praying Mantis – HARRICK) connected to an IR instrument (FTIR-Nicolet 6700 series). The total gas flow, 20 N cm^3/min, was kept constant. The outlet gases were analyzed by MS, the m/e values selected were the same studied in the TRM experiments. The catalyst was pre-treated with He at 500 °C during 1 h and activated *in situ* with H_2 at the same conditions. Reaction was carried out isothermally at 500 °C in an He-diluted stoichiometric feed (CH_4/CO_2/He). During the experiment the feed composition was temporarily changed from the reaction mixture to one of the reactants (CO_2–CH_4 → CH_4 → CO_2–CH_4 → CO_2). *In situ* activated catalyst was used as background and the characteristic signals related to CO and CH_4 gas phase have not been subtracted from the spectra. MS data were normalized, taking into account the maximum registered for each signal during the whole DRIFT-MS test.

3. Results and discussion

3.1. Characterization

Results from N_2 adsorption–desorption measurements indicate the significant difference, in terms of the morphological

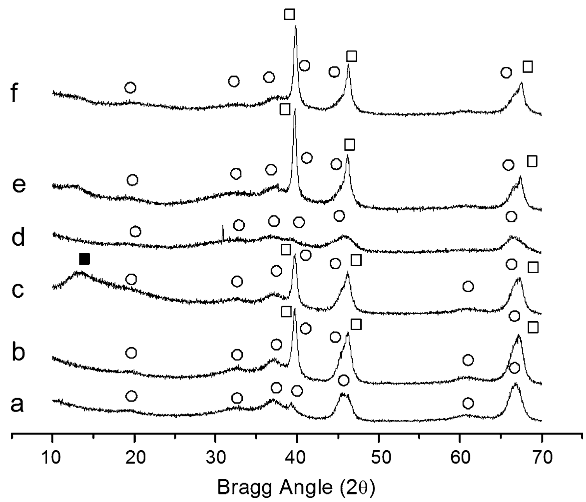

Fig. 1. XRD of supports and catalysts before (BR) and after reaction (AR). (a) γ-Al_2O_3(S); (b) Pt/γ-Al_2O_3(S) BR; (c) Pt/γ-Al_2O_3(S) AR; (d) γ-Al_2O_3(N); (e) Pt/γ-Al_2O_3(N) BR; (f) Pt/γ-Al_2O_3(N) AR; (○) γ-Al_2O_3; (□) Pt^0; (■) C.

characteristics, between the γ-Al_2O_3(S) and the γ-Al_2O_3(N) supports, where the A_{BET} and the V_P values of the γ-Al_2O_3(S) support are 50% less than those of the γ-Al_2O_3(N). No further modifications were registered for Pt-containing catalysts.

X-ray diffraction patterns are shown in Fig. 1. Both supports present the characteristic features of a γ-alumina (JCPDS 75-0921) and remain unchanged after reaction. In both of the catalysts, before and after reaction, Pt^0 was detected (JCPDS 01-1190) in agreement with XPS results. XRD pattern for the Pt/γ-Al_2O_3(S) catalyst, registered after reaction, reveals a broad signal centered at 13.6° (2θ), which is related to graphitic carbon (JCPDS 89-8491). The values of the biding energies of Pt $4d_{5/2}$ core electrons for both of the catalysts, before and after reaction, are presented in Table 1. Deconvoluting the Pt $4d_{5/2}$ region, the presence of two different Pt species was detected for the Pt/γ-Al_2O_3(S) catalyst, before and after reaction. The major component was registered at 314.4 eV; which indicates the presence of Pt^0 [2,17]. The second one was observed at 317.8 eV, this latter is related to the presence of Pt as PtO [18]. For the Pt/γ-Al_2O_3(N) catalyst, before reaction, two Pt components of Pt $4d_{5/2}$ were also detected; one with a signal centered at 314.7 eV associated to the presence of Pt^0 and another one located at 314.4 eV related to Pt as PtO. After reaction, only one Pt species at 314.2 eV was observed, which is characteristic of Pt^0. It is interesting to note that, for the nanofibrous alumina, the Pt^0 sites population is higher than that observed on the commercial alumina; that proportion increases after reaction. This observation suggests that the Pt interaction with the γ-Al_2O_3(N) support is different from that of the Pt with the γ-Al_2O_3(S) support.

Table 1
XPS results for Pt for both catalysts, before (BR) and after reaction (AR).

	Pt $4d_{5/2}$			
	Pt/γ-Al_2O_3(S)		Pt/γ-Al_2O_3(N)	
	BR	AR	BR	AR
Pt^0	314.4 (75)[a]	314.4 (88)	314.7 (85)[a]	314.2
PtO	317.8 (25)	317.8 (12)	317.4 (15)	
Pt/Al[b]	0.01	0.002	0.008	0.005

[a] Binding energies (±0.2 eV), in parentheses ( ) relative population of the species expressed in %.
[b] Pt/Al atomic ratios.

TEM images of supports and catalysts, before and after reaction, are shown in Fig. 2. It can be observed that there are morphological differences between supports: pseudo-amorphous and nanofibrous structure for the γ-Al_2O_3(S) and the γ-Al_2O_3(N), respectively. Furthermore, TEM images reveal that the Pt/γ-Al_2O_3(N) catalyst seems to have a better dispersion and homogeneity of Pt particle size than the Pt/γ-Al_2O_3(S), before and after reaction. In addition, it was calculated by the Scherrer equation that the average particle size of Pt is around 12 nm and 10 nm for the Pt/γ-Al_2O_3(S) and Pt/γ-Al_2O_3(N) fresh catalysts, respectively.

Crystallites of Pt with an average diameter of approximately 30 nm were observed in the γ-Al_2O_3(S) catalyst after reaction. On the other hand, the Pt/γ-Al_2O_3(N) catalyst after reaction does not show Pt sintering, keeping the average particle size value (10 nm). This observation together with the lower Pt^0 sites population observed by XPS for the γ-Al_2O_3(S) catalyst, confirms that the Pt interaction with the support is different for both of the catalysts.

The formation of mixed oxides of Pt and Al_2O_3 was not observed by XPS or XRD. This is contrary to what occurs with Ni-base catalysts supported on alumina, which tend to form mixed oxides that could inhibits the reducibility of Ni species [19,20].

3.2. Transient experiments

3.2.1. Experiments Type I (CH_4–He–Ar/CO_2–He–Ar)

The interaction between each reactant and the activated catalysts was analysed by the study of the cyclic response of a CH_4 rectangular pulse followed by a CO_2 pulse. The CH_4 signals detected by MS, for two subsequent cycles (two pulses of CO_2 and two of CH_4), are presented in Fig. 3. It can be seen that the CH_4 conversion reached higher values, in the temperature range studied, with the Pt/γ-Al_2O_3(N) catalyst. This was also reflected by the H_2 production obtained, as is shown in Fig. 4, which increased along with the temperature for both of the catalysts and it was higher for the Pt/γ-Al_2O_3(N) catalyst than for the Pt/γ-Al_2O_3(S).

It is worth noticing that the variation of the conversion values and H_2 production, between the Pt/γ-Al_2O_3(N) and the

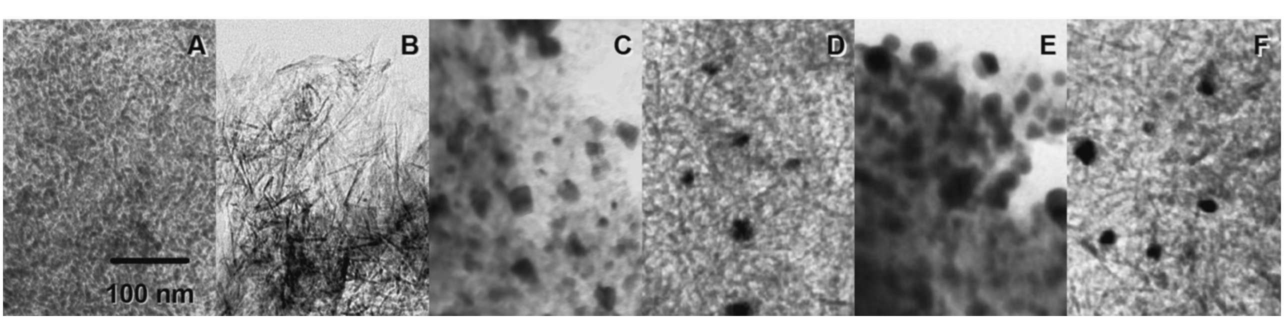

Fig. 2. TEM images of supports and catalysts before (BR) and after reaction (AR). (A) γ-Al_2O_3(S); (B) γ-Al_2O_3(N); (C) Pt/γ-Al_2O_3(S) BR; (D) Pt/γ-Al_2O_3(N) BR; (E) Pt/γ-Al_2O_3(S) AR; (F) Pt/γ-Al_2O_3(N) AR.

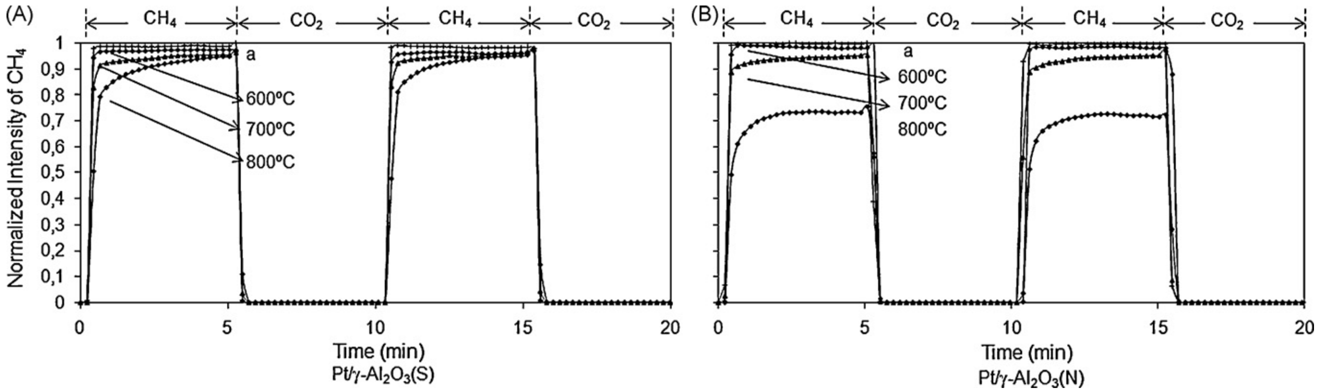

Fig. 3. MS profile of CH_4 for two consecutive cycles of the Experiments Type I (CH_4/CO_2). (a) CH_4 normalized signal registered at room temperature; (A) Pt/γ-Al_2O_3(S) catalyst; (B) Pt/γ-Al_2O_3(N) catalyst.

Pt/γ-Al_2O_3(S) catalysts, significantly increased with the temperature. The CH_4 conversion and consequently the rate of H_2 production were probably as a result of the methane cracking. The superficial acidity of the support or the number of electronic vacancies could have contributed to the increment of the activation level of CH_4. It has been reported that the catalysts' activity for the methane decomposition is correlated with the metal surface area and catalysts' acidity [21,22]. Additionally, in previous experiments (unpublished data), we have observed that the Pt^0/PtO ratios and the catalysts' activity in Pt-catalysts for dry reforming of methane, supported on diverse Al_2O_3 with different superficial characteristics, were influenced by the surface area and acidity of the support. This is in agreement with, Navarro et al. [23] who reported that the interaction between Pt and support or other metals produce changes in the Pt reducibility.

During the CH_4 pulse the presence of H_2, H_2O and CO was detected in the whole temperature range, although the H_2O and CO signals were very weak. Only at 800 °C were the (m/e) signals of H_2O and CO slightly significant, as can be observed in Fig. 5, where the product distribution registered by MS is shown. It can also be noticed that the H_2O and CO signals are more intense for the Pt/γ-Al_2O_3(N) catalyst than for the Pt/γ-Al_2O_3(S). Additionally, the CO profile, during the CH_4 pulse, shows a peak with a maximum value before the first minute that immediately decreases until it reaches the baseline. Moreover, a TRM experiment with CH_4 as the first pulse was done over a fresh and reduced catalyst (data not shown); CO production was not observed. These results together suggest that the CO, in the CH_4 pulses, could come from two sources: (i) from the surface carbon oxidation. This means that, after the CO_2 pulse, some oxygen could be over the catalyst surface that in contact with the carbon formed from the CH_4 activation, would form CO at the beginning of the CH_4 pulse; (ii) from the direct activation of the remaining CO_2, which is the most probable due to the shape of the CO signal during the CH_4 pulse. O'Connor et al. [3] performed a pumb-probe experiment over Pt/Al_2O_3 and Pt/ZrO_2, where a short CH_4 pulse followed by a $^{13}CO_2$ pulse was introduced into the reaction system. They registered the formation of CO and ^{13}CO, the first coming from the CH_4 dissociation and the subsequent reaction of the C with the surface oxygen species and the latter from the $^{13}CO_2$ activation.

Besides, for both catalysts the H_2 signal seems to be delayed with respect to the CO and CH_4 signals, which suggests the H_2 interaction with the catalysts' surface. This delay is more evident for the Pt/γ-Al_2O_3(S) catalyst than for the Pt/γ-Al_2O_3(N), moreover, it coincides with the appearance of the H_2O signal. The presence of H_2O indicates that CO_2 has been activated during the CO_2 pulse, replenishing with oxygen the catalyst surface. Additionally, the H_2O signal is delayed with respect to the H_2 signal for both of the catalysts. These results suggest that, the differences of the supports have influence on the catalytic behaviour.

On the other hand, during the CO_2 pulse, for both of the catalysts tails were detected on the CH_4, H_2 and H_2O signals, which indicates the desorption of the species after the CH_4 pulse. During this pulse, a CO production was also registered for both of the catalysts, which was higher for the Pt/γ-Al_2O_3(N) catalyst than for the Pt/γ-Al_2O_3(S). Furthermore, the CO_2 conversion values obtained in these tests, for both of the catalysts, were very low. Just at 800 °C were the CO_2 conversion values appreciable, 20% and 5% for the Pt/γ-Al_2O_3(N) and the Pt/γ-Al_2O_3(S) catalysts, respectively. This could be due to the low reduction level of the catalysts

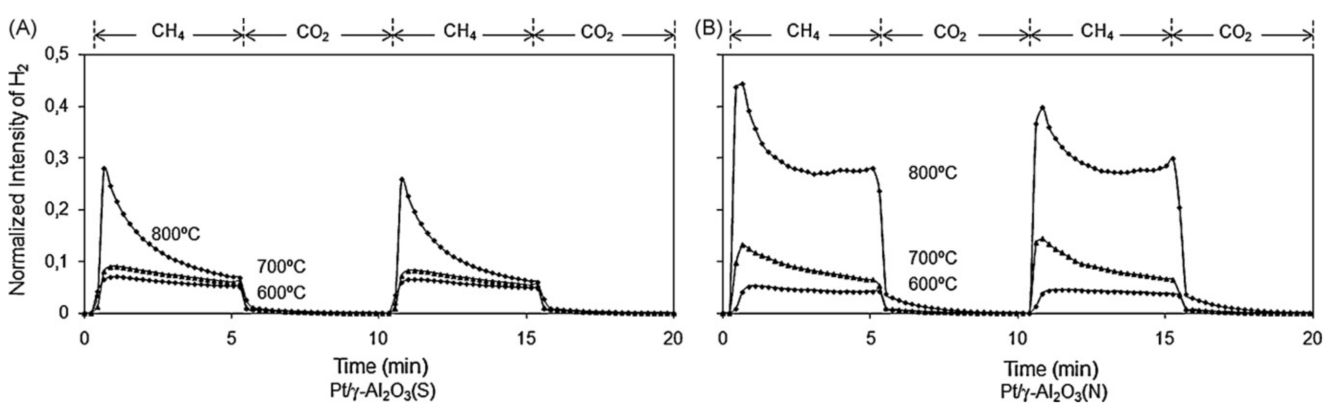

Fig. 4. MS profile of H_2 for two consecutive cycles of the Experiments Type I (CH_4/CO_2). (A) Pt/γ-Al_2O_3(S) catalyst; (B) Pt/γ-Al_2O_3(N) catalyst.

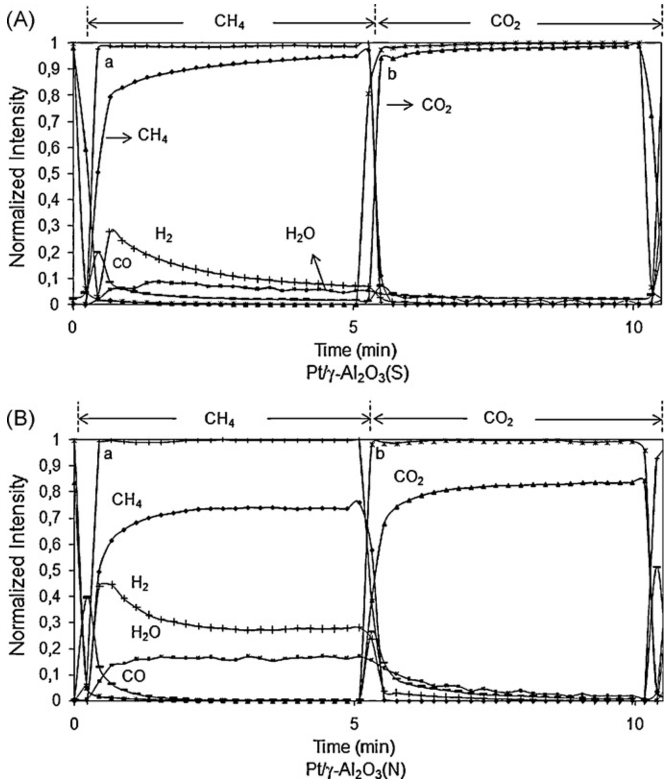

Fig. 5. MS profile during one cycle in the Experiments Type I at 800 °C. (A) Pt/γ-Al_2O_3(S) catalyst; (B) Pt/γ-Al_2O_3(N) catalyst; (a and b) CH_4 and CO_2 normalized signals registered at room temperature.

during the end of the CO_2 pulse. It is well established that the CO_2 activation depends on the reduction level of the catalyst and it is minimal in poor H_2 atmospheres. Solymosi et al. [24] suggested that the CO_2 activation is promoted by H_2. O'Connor et al. [3] reported that for a Pt/Al_2O_3 catalyst which was subjected to CO_2 multipulses, the production of CO was minimal. Moreover, Maestri et al. [13] reported that the CO_2 adsorption over the catalyst surface and its activation is due to hydrogen adsorbed. This could explain the significant difference between the CO_2 conversions obtained at 800 °C for both of the catalysts during the CO_2 pulse, where the H_2 produced with the Pt/γ-Al_2O_3(N) catalyst was appreciably higher than that with the Pt/γ-Al_2O_3(S). Additionally, it can be observed that the profile of the CO_2 signal during the CO_2 pulse changes after the disappearance of the H_2 tail. The CO_2 consumption was higher in the presence of H_2 than in the rest of the pulse, indicating the occurrence of two kind of CO_2 activation.

Results from Experiments Type I suggest the presence of two different types of CO_2 activation: (i) CO_2 activation promoted by H_2 or CH_4-species retained over the catalysts' surface, which principally occurs at the beginning of the CH_4 and CO_2 pulses; (ii) direct CO_2 activation over Pt, which occurs during the whole CO_2 pulse.

3.2.2. *Experiments Type II (CH_4–CO_2–He–Ar/He)*

These cyclic tests were performed introducing CH_4–CO_2 pulses into the reaction system, alternated with He pulses. The normalized MS profile of CH_4 for two cycles (two consecutive pulses of CO_2–CH_4 and two of He) is shown in Fig. 6. It can be observed that the CH_4 conversion values reached during these experiments were higher than those obtained during the Experiments Type I. This is probably due to the co-presence of CO_2, which could inhibit CH_4 cracking and promote the CH_4 reforming. It is further interesting to observe that the CH_4 conversion increased with the temperature for both of the catalysts.

The MS profile of H_2 for both of the catalysts, in the temperature range studied, is presented in Fig. 7. It could be noted that both of the catalysts were active for CO_2 reforming of methane and the H_2 production increased with the temperature, which at 800 °C was considerably higher for the Pt/γ-Al_2O_3(N) catalyst than for the Pt/γ-Al_2O_3(S). This result indicates the strong influence of the support on the catalyst performance over 700 °C.

The relative conversion values calculated from the area under the curve of the normalized intensity of the CO_2 and CH_4 signals are shown in Table 2. It can be observed that, for both of the catalysts, the CO_2 conversion values were higher than those of CH_4. This can be explained by the occurrence of parallel reactions as: reverse water gas shift reaction (RWGS), Boudouard reaction and carbon gasification. These results are in agreement with those obtained in the steady-state experiments, where the same trend was observed. Furthermore, the CO_2 and CH_4 conversion values in both of the experiments, Type II (Table 2) and steady-state (Table 3), were higher for the Pt/γ-Al_2O_3(N) catalyst than for the Pt/γ-Al_2O_3(S), which indicates that the Pt/γ-Al_2O_3(N) catalyst has a better behaviour under CO_2 reforming conditions. This was also confirmed by the H_2/CO ratios found in the steady-state experiments, where for the Pt/γ-Al_2O_3(N) catalyst the values of the H_2/CO ratios obtained were higher and closer to the thermodynamic ones than those for the Pt/γ-Al_2O_3(S).

Additionally, it is important to point out that comparing the results obtained in the Experiments Type II with the ones registered in the Experiments Type I, an increase of 96 and 79% was observed in the CO_2 conversions values for the Pt/γ-Al_2O_3(S) and Pt/γ-Al_2O_3(N) catalysts, respectively. This indicates that the presence of H_2 and CH_X species promotes the CO_2 activation.

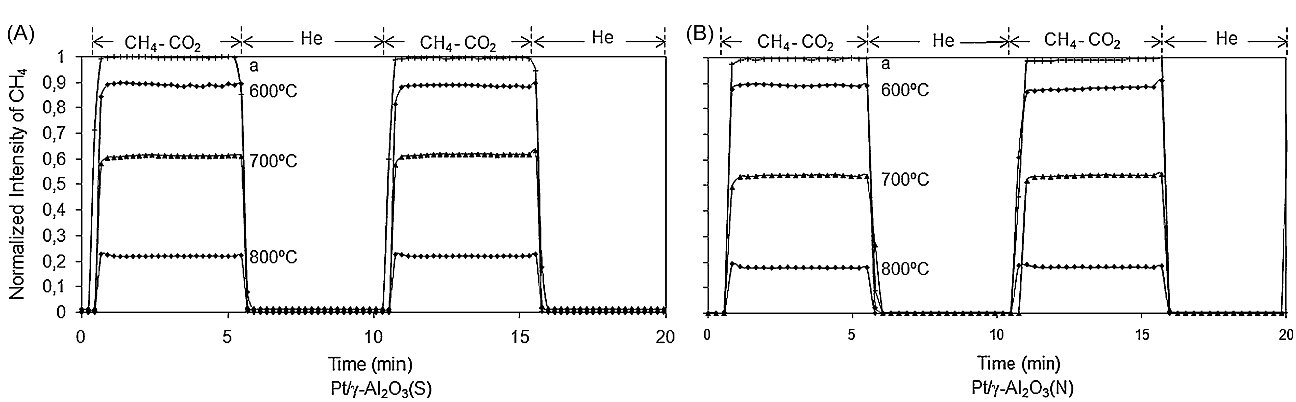

Fig. 6. MS profile of CH_4 for two consecutive cycles of the Experiments Type II (CH_4–CO_2/He). (a) CH_4 normalized signal registered at room temperature; (A) Pt/γ-Al_2O_3(S) catalyst; (B) Pt/γ-Al_2O_3(N) catalyst.

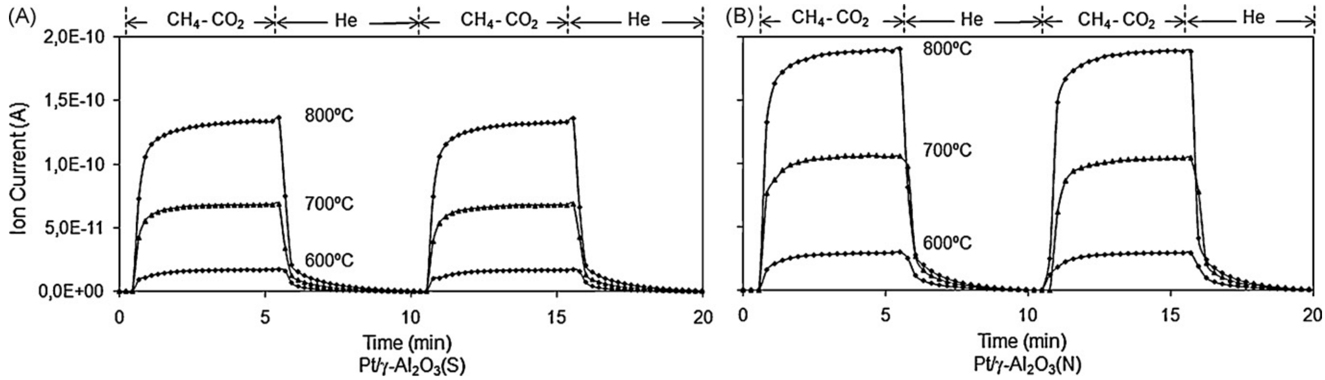

Fig. 7. MS profile of H_2 for two consecutive cycles of the Experiments Type II (CH_4–CO_2/He). (A) Pt/γ-Al_2O_3(S) catalyst; (B) Pt/γ-Al_2O_3(N) catalyst.

The normalized (m/e) signals detected by MS for both of the catalysts at 800 °C are shown in Fig. 8. During the CO_2–CH_4 pulse H_2, CO and H_2O were principally detected. Besides, during the He pulse the (m/e) signals registered were weak and originated from the desorption of the catalysts' surface species. From these results, it is interesting to note that, during the CO_2–CH_4 pulse, the CO and H_2 productions for both of the catalysts were simultaneous, which suggests that CO_2 and CH_4 activation are nearly contemporaneous. However, the CO signal reached its maximum earlier than the H_2 signal; this delay in the H_2 signal indicates that there is an H_2 interaction with the catalyst surface, which could rehydrogenate the surface or reduce the Pt species to Pt^0 to produce water (RWGS reaction). In addition, for both of the catalysts, the H_2O (m/e) signal was delayed in relation to the others (m/e) signals, suggesting that the H_2O formed at the begging is also used to hydrate the catalysts' surface or for steam gasification of the carbon formed.

Nevertheless, during the He pulse, desorption profiles of H_2 and H_2O were observed for both of the catalysts, where the desorption rates for the Pt/γ-Al_2O_3(N) were apparently higher than for the Pt/γ-Al_2O_3(S). This is probably associated to the superficial differences between both of the supports.

3.3. DRIFT-MS experiment

The DRIFT spectra obtained for the Pt/γ-Al_2O_3(N) catalyst at 500 °C are presented in Fig. 9. During this experiment the composition of the feeding gases was cyclical, changed from the reaction mixture to one of the reactants: CO_2–CH_4 (cycle 1, 15 min) → CH_4 (Cycle 2, 15 min) → CO_2–CH_4 (Cycle 3, 15 min) → CO_2 (Cycle 4, 30 min).

During the first cycle CO_2 and CH_4 were co-fed into the reaction system. Two bands, in addition to the bands due to CO_2 and CH_4 gas phase (2380–2309 cm^{-1} and 3016 cm^{-1}), were principally observed at the beginning of this period. Firstly, a strong band at 2057 cm^{-1}, which corresponds to CO linearly adsorbed. Secondly, a shoulder centred at 1980 cm^{-1}, which can be assigned to CO adsorption, shifted by the increase of the electronic density in the d subshell of Pt and promoted by the presence of H_2 and CH_X species [25,26]. The H_2 and the CH_X species come from the H adsorbed over the catalyst surface during the H_2 pretreatment and from the CH_4 activation. CO adsorption over the fresh catalyst (without H_2 pre-treatment) at 500 °C was done, and a unique band at 2057 cm^{-1} associated to CO over Pt was observed (data not shown).

After 15 minutes' exposure to CO_2–CH_4, together with the gas phase and the CO-adsorbed bands, weak bands associated to

Table 2
CH_4 and CO_2 conversion values obtained in the Experiments Type II (CH_4–CO_2/He).

T (°C)	Pt/γ-Al_2O_3(S)		Pt/γ-Al_2O_3(N)	
	XCH_4[a] (%)	XCO_2[b] (%)	XCH_4 (%)	XCO_2 (%)
600	8.0	10.5	10.5	13.8
700	36.7	47.3	45.6	59.4
800	77.0	96.8	82.1	95.4

[a] CH_4 conversion.
[b] CO_2 conversion.

Table 3
Reactivity results obtained in the steady-state experiments for the Pt/γ-Al_2O_3(S) and the Pt/γ-Al_2O_3(N) catalysts.

T (°C)	Pt/γ-Al_2O_3(S)			Pt/γ-Al_2O_3(N)		
	XCH_4[a] (%)	XCO_2[b] (%)	H_2/CO[c]	XCH_4 (%)	XCO_2 (%)	H_2/CO
550	11.7	15.1	0.38	15.4	21.0	0.48
600	17.7	23.1	0.53	23.4	30.6	0.59
650	25.3	32.6	0.60	41.6	54.2	0.64
700	44.6	56.0	0.64	65.5	76.1	0.68

[a] CH_4 conversion.
[b] CO_2 conversion.
[c] H_2/CO ratio.

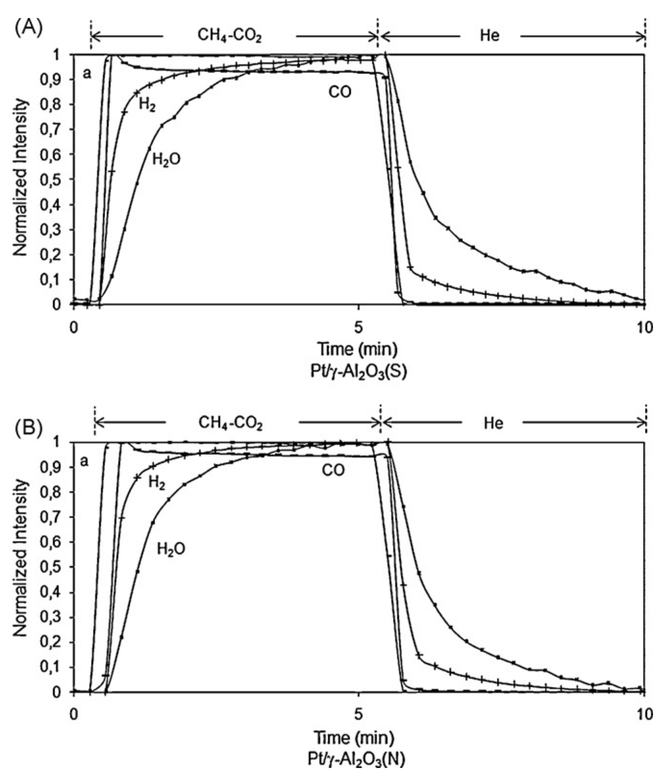

Fig. 8. MS profile for one cycle of the Experiments Type II at 800 °C. (A) Pt/γ-Al_2O_3(S) catalyst; (B) Pt/γ-Al_2O_3(N) catalyst; (a) Ar normalized signal.

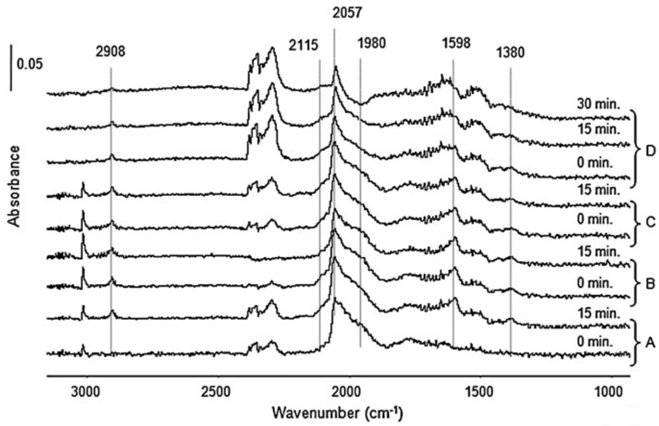

Fig. 9. DRIFT spectra registered *in situ* for the Pt/γ-Al_2O_3(N) catalyst under cyclic flow conditions at 500 °C. The sequence is from the bottom upwards. (A) Cycle 1 (CO_2–CH_4); (B) Cycle 2 (CH_4); (C) Cycle 3 (CO_2–CH_4); (D) Cycle 4 (CO_2).

formate species (1380, 1598 and 2908 cm^{-1}), CO gas phase (2115 cm^{-1}), carbonate, bicarbonate and carboxylate species (overlapped signals in the 1200–1770 cm^{-1} region) were registered. The MS profile obtained during Cycle 1 is presented in Fig. 10A. It can be noticed that H_2 and CO signals achieved their maximum after 1 min of reaction. However, the signals immediately diminished over time, reaching steady state at the end of the cycle. Another interesting observation is that the CO profile presents a shoulder after 2 min and it coincided with the H_2 consumption and the appearance of H_2O. The H_2O signal diminished progressively over time, as did the CO and H_2 signals.

During the next cycle, when only CH_4 was introduced, the CO_2 gas phase bands disappeared and the rest of them were kept over the catalyst surface. It is further interesting to observe that, the intensity of the shoulder centred at 1980 cm^{-1} increased, which is consistent with the previous band assignment. Additionally, a fast CH_4 consumption was observed by MS (Fig. 10B). Therefore, the CH_4 conversion increased and consequently the H_2 production also increased at the beginning of the cycle, although, after two minutes' exposure to CH_4, the H_2 signal constantly decreased. CO and H_2O were also detected during this cycle; however, the CO intensity diminished (50%) with respect to the previous cycle and H_2O signal constantly diminished until it reached the baseline level. The CO observed during this cycle could be a product of CO desorption from the last cycle (as was registered during the He pulse in the Experiment Type I) or also of the reaction between the remaining CO_2 over the catalyst surface and the C produced by the CH_4 cracking.

When CO_2 and CH_4 were subsequently fed into the reaction system (Cycle 3), all the bands observed during the first cycle were restored after less than 1 min of this cycle. The DRIFT spectra obtained and the data followed by MS at steady state were identical to those registered during Cycle 1. From the MS results (Fig. 10C), it can be observed that after 2 min of Cycle 3 H_2, CO and H_2O intensities were similar to those registered at the end of the Cycle 1.

Finally, when the catalyst was only exposed to CO_2, at the beginning of the cycle, the bands of the CH_4 gas phase disappeared. The intensity of the bands associated to formate species and CO-promoted adsorption diminished, while that related to carbonate and bicarbonate species increased. After 15 min, the shoulder at 1980 cm^{-1} and the bands related to formate species practically disappeared. At the same time, the H_2 signal followed by MS almost reached the zero point and the CO line continuously diminished (see Fig. 10D). The disappearance of the shoulder at 1980 cm^{-1}, confirms the previous assignment of CO adsorption promoted by CH_X species and H_2. Furthermore, the intensity of the band at 2047 cm^{-1}, assigned to linearly adsorbed CO, was lower

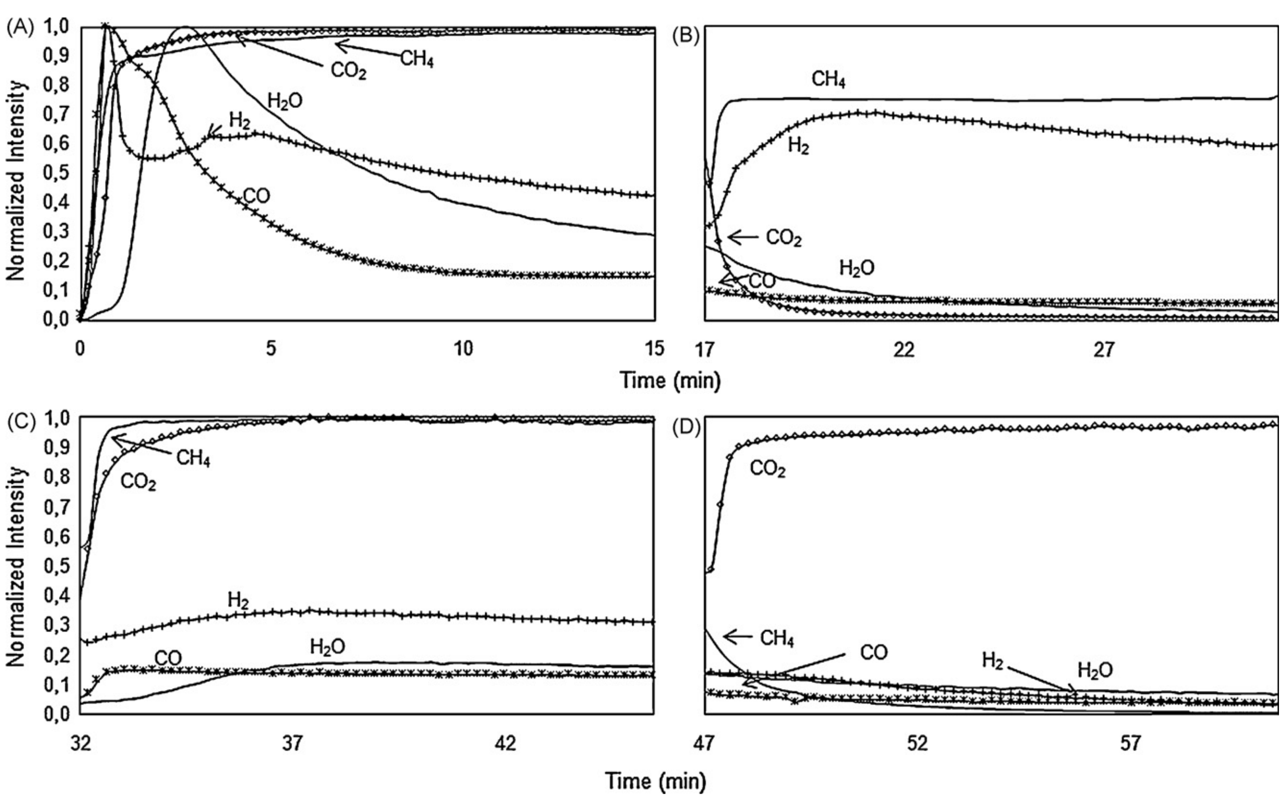

Fig. 10. MS profile obtained during the DRIFT-MS test for the Pt/γ-Al_2O_3(N) catalyst under cyclic flow conditions at 500 °C. (A) Cycle 1 (CO_2–CH_4); (B) Cycle 2 (CH_4); (C) Cycle 3 (CO_2–CH_4); (D) Cycle 4 (CO_2).

than in the periods where CH_4 was fed into the system. This result, together with the disappearance of the shoulder at 1980 cm^{-1} and the diminution of the CO production, indicates that the presence of H_2 and CH_X species enhances the CO_2 activation, as was observed in the TRM experiments.

The formate species could be as a product of the reactive coadsorption of H_2 and CO_2 or of the reactive adsorption of CO on a wet or highly hydroxylated alumina surface [27]. Because of that the formate species disappeared when the H_2 production during the Cycle 4 was negligible, allowing the growth of bicarbonate ions over the catalyst surface, as a consequence of the reaction of CO_2 with the hydroxyl groups of the support.

An important observation is that the reactants are activated over the catalyst surface during each feeding cycle. This is also supported by the results obtained by MS, where H_2 and CO production was registered when CH_4 or CH_4–CO_2 were fed into the reaction system; and CO when only CO_2 was introduced.

The results obtained suggest that CH_4 and CO_2 are activated independently over the catalyst surface during the periods where each reactant is fed separately. When reactants are introduced simultaneously, apart from the formation of formates, carboxilates and bicarbonates species, there is a CO_2 activation process, which is promoted by the CH_X species. This process is responsible for the production of H_2 + CO and probably requires the presence of easily reducible Pt particles with a good dispersion. The surface reaction between CH_X-adsorbed species and the O-adsorbed species could be rate-controlling of the dry reforming of methane.

4. Conclusion

The morphological differences between the catalyst supports affect in general the catalyst performance under given reaction conditions. Over both of the catalysts Pt is present as Pt^0, with a higher dispersion and stability in the case of the Pt supported on a nanofibrous alumina, which presents a better behaviour in terms of reactivity. It was found that CH_4 and CO_2 molecules are activated over the catalysts' surface. However, when the reactants are introduced simultaneously into the reaction system, CO_2 activation is promoted by the CH_X species, which probably initiates the reforming reaction.

Acknowledgements

MGD acknowledges the Spanish Minister of Education and Science for a FPI grant and for the financial support of the projects ENE2004-06176 and ENE2007-67926-C02-02/ALT.

References

[1] F. Pompeo, N.N. Nichio, M.M.V.M. Souza, D.V. Cesar, O.A. Ferretti, M. Schmal, Appl. Catal. A 316 (2007) 175.
[2] B. Pawelec, S. Damyanova, K. Arishtirova, J.L.G. Fierro, L. Petrov, Appl. Catal. A 323 (2007) 188.
[3] A.M. O'Connor, Y. Schuurman, J.R.H. Ross, C. Mirodatos, Catal. Today 115 (2006) 191.
[4] P. Ferreira-Aparicio, C. Márquez-Álvarez, I. Rodríguez-Ramos, Y. Schuurman, A. Guerrero-Ruíz, C. Mirodatos, J. Catal. 184 (1999) 202.
[5] M. Rezaei, S.M. Alavi, S. Schedelfar, Z.-F. Yan, J. Catal. 15 (2006) 327.
[6] J.M. Wei, B.Q. Xu, J.L. Li, Z.X. Cheng, Q.M. Zhu, Appl. Catal. A 196 (2000) L167.
[7] J. Wei, E. Iglesia, J. Catal. 224 (2004) 370.
[8] A.D. Ballarini, S.R. de Miguel, E.L. Jablonski, O.A. Scelza y, A.A. Castro, Catal. Today 107–108 (2005) 481.
[9] J.H. Bitter, K. Sesham, J.A. Lercher, J. Catal. 171 (1997) 279.
[10] H.Y. Wang, E. Ruckenstein, Appl. Catal. A 204 (2000) 143.
[11] M. García-Diéguez, M.C. Herrera, M.A. Larrubia, I.S. Pieta, I. Malpartida, L.J. Alemany, Proc. XXI Simposio Iberoamericano de Catálisis (SICAT), Málaga, Spain, June 22–27, (2008), p. 229.
[12] C.J. Michael, M. Bradford, A. Vannice, J. Catal. 173 (1998) 157.
[13] M. Maestri, D.G. Vlachos, A. Beretta, G. Groppi, E. Tronconi, J. Catal. 259 (2008) 211.
[14] Y. Schuurman, C. Márquez-Álvarez, V.C.H. Kroll, C. Mirodatos, Catal. Today 46 (1998) 185.
[15] A. Olafsen, Å. Slagtern, I.M. Dahl, U. Olsbye, Y. Schuurman, C. Mirodatos, J. Catal. 229 (2005) 163.
[16] H.Y. Zhu, J.D. Riches, J.C. Barry, Chem. Mater. 14 (2002) 2086.
[17] J.Z. Shyn, K. Otto, Appl. Surf. Sci. 32 (1988) 246.
[18] J. Escard, B. Pontvianne, M.T. Chenebaux, J. Cosyns, Bull. Soc. Chim. Fr. 11 (1975) 2400.
[19] K.Y. Koo, H.-S. Roh, Y.T Seo, D.J. Seo, W.L. Yoon, S.B. Park, Appl. Catal. A 340 (2008) 183.
[20] N. Sahli, C. Petit, A.C. Roger, A. Kiennemann, S. Libs, M.M. Bettahar, Catal. Today 113 (2006) 187.
[21] J. Ashok, M. Subrahmanyan, A. Venugopal, Catal. Surv. Asia 12 (2008) 229.
[22] Y. Li, B. Zhang, X. Xie, J. Liu, Y. Xu, W. Shen, J. Catal. 238 (2006) 412.
[23] R.M. Navarro, M.C. Álvarez-Galván, F. Rosa, J.L.G. Fierro, Appl. Catal. A 297 (2006) 60.
[24] F. Solymosi, Gy. Kutsan, A. Erdohelyi, Catal. Lett. 11 (1991) 149.
[25] A.V. Kiselev, V.I. Lygin, Infrared Spectra of Adsorbed Species, Academic Press, London/New York, 1966, p. 206.
[26] E.V. Benvenutti, L. Franken, C.C. Moro, Langmuir 15 (1999) 8140.
[27] G. Busca, V. Lorenzelli, Mater. Chem. 7 (1982) 89.